Rheology at the Phase Transition Boundary: 2. Hexagonal Phase of Triton X100 Surfactant Solution

S. V. Ahir,† P. G. Petrov,‡ and E. M. Terentjev*

Cavendish Laboratory, University of Cambridge, Madingley Road, Cambridge CB3 0HE, United Kingdom

Received April 1, 2002. In Final Form: June 17, 2002

The phase behavior of the Triton X100/water binary mixture is investigated using rheological, optical, and X-ray synchrotron techniques. In particular, the storage shear modulus G' response, as a function of temperature and strain amplitude, has been related to the structural transformation into the hexagonal phase of cylindrical micelles. Results demonstrate a characteristic critical behavior at the phase transition boundary $T = T_c$. However, we also find that the rheological signature of the ordering phase transition crucially depends on the particular dynamical mode applied to the sample. Stress−strain variation reflects the shear-induced alignment of the principle column axis, which results in the two-dimensional melting of hexagonal order and the onset of creep flow above a threshold strain ϵ^*.

1. Introduction

Complex fluid systems such as surfactant/water combinations have been intensely and systematically studied for many years now. Industrially, surfactant products,[1] such as detergents and emulsions, continually experience varied and sometimes unpredictable shear regimes; despite a number of great advances, we are still unable to command their full understanding. Beyond manufacturing interests, surfactant/water systems also have clear implications in the biology of cell membranes[2] and relating their structural and rheological properties may well lead to advances at the life science interface.

Above a certain critical concentration, amphiphilic surfactant molecules aggregate in solution to form nanosized spherical micelles; further increasing the concentration leads to the formation of cylindrical micelles which in turn occupy the relative crystallographic points of a hexagon. Unlike solid hexagonal structures, lyotropic liquid crystals demonstrate only two-dimensional order[3] but are able to simultaneously convey long-range orientational order characterized by the orientation of the cylinder axis, called, in this context, a director. However, on a macroscopic scale, uniform alignment does not occur, thus leading to the well-recognized polydomain structure.[4−6]

Although many studies of complex fluid rheology have been carried out over the years, surprisingly little work has taken place to connect the observed rheological data to the actual ordered structure, in particular, with hexagonal phases. Though some important efforts were made by Wolff et al.[7] and Dimitrova et al.,[8] a gap still remains in our understanding of material behavior in and around the phase transition region. This is further complicated by the fact that our choice of surfactant, Triton X100,[9] is often mistaken for a linear viscoelastic material when in fact it is not. The X100 surfactant phase diagram in a binary mixture with water is shown in Figure 1. The wide commercial availability of this surfactant and the ease with which the hexagonal phase can be isolated makes it an obvious choice upon which to experiment.

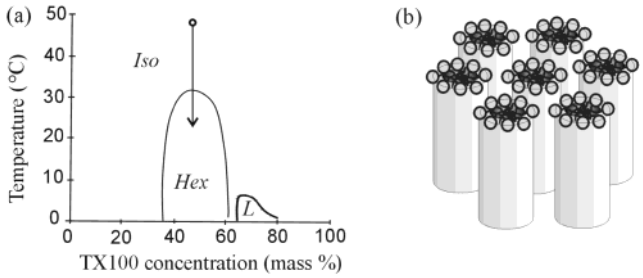

Figure 1. (a) Schematic phase diagram of the TX100−water binary system, from ref 9. The main ordered phase is the hexagonal, see the sketch in (b), with a pocket of lamellar phase at low temperature and high concentrations. The diagram does not distinguish between the isotropic colloidal phase of spherical surfactant micelles and the homogeneous mixture below the critical micelle concentration.

Though this paper briefly addresses director orientation and shear-induced transitions (for which Schmidt et al.[5] and Ramos et al.[6] have accounted well), it more importantly demonstrates certain novel rheological results as the sample follows different temperature profiles. This aspect of the phase behavior is novel in itself and can further be used to initiate an understanding of what mechanisms are taking place during the first-order phase transition between the isotropic mixture of spherical micelles and the hexagonally ordered cylinders. A connection is made between our results and the theoretical arguments set up by previous work.

Of clear interest to us is the role the microstructure plays in the overall scheme of the mechanical behavior in

* To whom correspondence should be addressed. E-mail: emt1000@cam.ac.uk.

† Present address: Imperial College of Science, Technology and Medicine, London SW7 2AY.

‡ Present address: Department of Physics, University of Exeter, EX4 4QL.

(1) Terry, A. E.; Odell, J. A.; Nicol, R. J.; Tiddy, G. J. T.; Wilson, J. E. *J. Phys. Chem. B* **1999**, *103*, 11218.

(2) Israelachvili, J. *Intermolecular and Surface Forces*; Academic Press: London, 1992.

(3) Imperor-Clerc, M.; Davidson, P. *Eur. Phys. J. B* **1999**, *9*, 93.

(4) Ramos, L.; Molino, F. *Europhys. Lett.* **2000**, *51*, 320.

(5) Schmidt, G.; Müller, S.; Lindner, P.; Schmidt, C.; Richtering, W. *J. Phys. Chem. B* **1998**, *102*, 507.

(6) Ramos, L.; Molino, F.; Porte, G. *Langmuir* **2000**, *16*, 5846.

(7) Klaussner, B.; Wolff, T. *J. Surf. Sci. Technol.* **1992**, *8*, 407.

(8) Dimitrova, G. T.; Tadros, Th. F.; Luckham, P. F. *Langmuir* **1995**, *11*, 1101.

(9) Beyer, K. *J. Colloid Interface Sci.* **1982**, *86*, 73.

10.1021/la025793c CCC: $22.00
Published on Web 10/29/2002

this system. In particular, the function of defects in the hexagonal phase as characterized by Sallen et al.[10] is of great interest and therein, related to some of the results we have obtained. The effect of undulations of cylindrical micelles in the mesophase is also of some importance and is briefly considered. However, though we would like to take this up further, the present theories themselves seem speculative at best and further work is required if experimental phenomena are to be related to such ideas.

The purpose of this work has been to investigate the effect of heating/cooling rates on the mechanical response (given by the storage shear modulus G') of a hexagonal phase. In addition, dynamic strain experiments are carried out at various temperatures to help develop the relationship between the stress and the strain amplitude, which is clearly nonlinear. These data allow conclusions to be made regarding the alignment processes occurring during application of shear forces. Small-angle synchrotron X-ray experiments were also conducted to provide confirmation of lattice parameters and nanoscale descriptions of the structural integrity at various temperatures. Images from ordinary polarized microscopy and confocal microscopy provide an additional description of textures emerging at the phase transition. Overall, unusual and novel results are presented and discussed.

Understanding the rheological and phase behavior of hexagonal phases is of both scientific and commercial interest. It is hoped that this paper contributes to that understanding and presents work that could nurture its growth.

2. Experimental Section

2.1. System. The nonionic surfactant used was Triton X100 (TX100) (poly(ethylene glycol)-*tert*-octylphenyl), a widely available commercial product obtained by the ethoxylation of *p*-(1,1,3,3-tetramethylbutyl)phenol containing an average number of 9.5 oxyethylene units per molecule.[11] This batch was obtained from Aldrich Chemical Corp. and used without any further purification. Distilled water was then added at room temperature (at a fixed proportion of 50 wt % TX100/50 wt % water). This formed the desired material with a hexagonal phase in the range of 5−32 °C. The batch was then mixed by a IKAMAG RCT magnetic stirrer for an hour, set at 60 Hz and 50 °C. This ensured full mixing and homogeneity throughout the sample.

2.2. Rheometer. Rheological measurements were staged on a stress-controlled Rheometrics DSR (dynamic stress rheometer) connected to a water bath heater, an acceptable source as our working range lay between 5 and 60 °C. A cone and plate geometry (25 mm, 0.1 rad) was utilized as clearly this ensures a consistent shear rate in the total volume of the liquid.[12] An added precaution was to keep the distance between the cone tip and the bottom plate relatively small at $55 \pm 5\,\mu$m ensuring that a homogeneous shear stress was experienced throughout the sample. Finally, the sample perimeter was carefully coated with low-viscosity silicone oil to prevent solvent loss or atmospheric moisture absorption. Initial experimentation showed this dehydration to have a significant impact on results; hence all samples including those tested at temperatures <15 °C were lined with silicone oil.

The main batch of sample was contained in an airtight bottle, and specimens to be tested were removed using a clean spatula. Great care was taken to ensure that no undue disturbance was experienced by the samples, and at the very least, all samples underwent the same treatment history before loading into the rheometer. We appreciate the effect stress history can have on liquid crystal specimens, as stated in this context by ref 8, but decided that all samples should nevertheless be presheared to instate a uniform starting condition. Therefore, all tests were carried out using fresh samples which were presheared in the rheometer with a stress of 10 Pa while kept in the isotropic phase at 50 °C. When the mesophase is heated to an isotropic solution, all previous orientation is removed while the concentration remains unchanged due to the presence of silicone oil around the boundary.

The first series of rheological experiments involved observing hexagonal phase behavior as the sample was cooled and heated at different rates. Measurements were performed under low-amplitude oscillatory shear, at a relatively low frequency of 1 Hz (making the shear rate $\dot{\epsilon} \sim 0.01\ s^{-1}$), with an initial applied stress of 1 Pa. We discuss at some length, in section 4.2, that there is essentially no linear stress−strain regime in the hexagonal lyotropic phase: the choice of strain rate is therefore somewhat arbitrary, dictated by comparison with other complex fluid systems where at $0.01\ s^{-1}$ one expects little disturbance to the microstructure. Samples were presheared at 50 °C, cooled to around 15 °C at various rates, and then heated back up to the isotropic phase, above 50 °C. The variation of the storage modulus (G') with temperature was examined throughout.

In these experiments, the main difficulty is to obtain a continuous signal when the system undergoes a rapid transition from a liquid to an essentially solid state, changing the effective shear modulus by at least 7 orders of magnitude. To achieve this, the strain amplitude was set using the rheometer control software to be automatically kept between 1.25 and 1.5%. Maintaining the strain amplitude on a stress-controlled rheometer requires automatic stress adjustment. This adjustment is achieved by a stepwise increment of the torque applied to the shear cell, until the returned measured strain achieves its target value. This procedure should be contrasted with a response on a genuinely strain-controlled rheometer, where a fixed amplitude of shear strain applied to the sample returns different values of measured torque and, thus, stress. We discuss this issue at some length in section 4.1, compare the results provided by the two different approaches to rheometry, and discuss their applicability and physical meaning.

The second series of rheological experiments required direct observation of the variation of G' with strain amplitude for the hexagonal phase material. Again, the samples were presheared at relatively high temperatures and then cooled slowly to the testing temperature. Once equilibrated, a constant static force is applied (frequency = 1 Hz) to provide a strain increase in intervals of 0.5% up to 60% and the G' response is recorded.

As a control experiment, we also carried out studies on a strain-controlled rheometer, ARES from Rheometric Scientific, the access to which was kindly provided by King's College London. The true strain control allows the fixed amplitude of imposed oscillating shear to be imposed on the sample irrespective of structural and rheological changes that take place in it. In the main body of this article, we shall compare the two results and discuss at some length which of the two methods gives more physically appropriate results.

2.3. X-ray Diffraction. Small-angle X-ray diffraction (SAXS) studies were performed at station 8.2 of the synchrotron radiation source at Daresbury Laboratory, Cheshire, U.K. The small angle detector camera length was set between 1.5 and 3.5 m, thus providing the scattering vector values in the range of 0.05−0.30 $Å^{-1}$. Samples were held between a mica sheet of 0.1 mm and an aluminum plate (mica supplied by Goodfellow, Cambridge, U.K), with a brass spacer of 0.25 mm thickness. The metal substrate plate was used to ensure accurate heat transfer to and from the sample. Sample temperature was controlled by a Lauda water-bath and verified by the Linkam TP91 hot stage unit. Three different samples from the same batch (50 wt % X100 and water) were tested using the setup mentioned above. The hexagonal lattice spacing, a, was calculated from the diffraction data using simple crystallographic arguments.

2.4. Differential Scanning Calorimetry (DSC). A Perkin-Elmer power-compensated Pyris 1 differential scanning calorimeter equipped with an Intracooler 2P was used. To focus on the isotropic−hexagonal phase transition, samples were heated to 45 °C, held for 15 min, cooled to 25 °C at a specified rate, held for 15 min, and then reheated to 45 °C at the same rate. The

(10) Sallen, L.; Sotta, P.; Oswald, P. *J. Phys. Chem. B* **1997**, *101*, 4875.
(11) Galatanu, A. N.; Chronakis, I. S.; Anghel, D. F.; Khan, A. *Langmuir* **2000**, *16*, 4922.
(12) Léon, A.; Bonn, D.; Meunier, J.; Al-Kahwaji, A.; Kellay, H. *Phys. Rev. Lett.* **2001**, *86*, 938.

experiment was then repeated at a different temperature rate with the same sample, and transition temperatures were extrapolated to the zero cooling rate, which was perceived as the equilibrium value.

2.5. Hot Stage Optical Microscopy. A Zeiss Axioplan microscope with cross polarizers was attached to a Linkam TP91 hot stage unit. Samples of the Triton X100/water binary system were placed between thin microslides (all slides were washed in acetone before use). The bottom slide contained a spherical cut-out/basin in its center where the material could lie and then be covered by the top slip. Material in the center of the bowl was therefore not in contact with the glass on either the top or bottom plate, thus reducing the effect of shearing due to contact with the glass. All images taken represent material from this region of the sample. The samples were heated above the transition temperature (36 °C) and kept at this temperature for 10 min. They were then cooled at specified and well-controlled rates with pictures taken at significant points before, during, and after the nucleating period.

2.6. Shear Stage Confocal Microscopy. A Zeiss LSM 510 confocal microscope was used to provide more three-dimensional images of the binary system. A Linkam shear stage CSS450 device was also attached in an attempt to reproduce the conditions set up in the rheological study. Samples were sheared at 10 Pa while in the isotropic liquid phase (around 50 °C) to remove any stress history. They were then cooled, with pictures being taken from 33 °C at 30 s intervals until the hexagonal phase was well established at 29 °C. The cooling rate was not accurately controlled due to the limitations of the shear stage equipment, and thus the samples were cooled at an ambient rate. During the cooling cycle, a constant strain amplitude of 1.5% was maintained at a frequency of 1 Hz.

3. Structural Transformation

In this section, we first examine the equilibrium properties of the hexagonal phase and its phase transition without any applied stress.

3.1. Phase Transition and Textures. Evidence of phase transitions of the binary Triton X100/water system is well established by the work of Marsden,[13] Ekwal,[14] and more recently Beyer.[9] However, in light of recent more sensitive techniques, it was of interest to revisit a well-known system and try to map the structural behavior in the phase transition region. Establishing the point at which the phase transition occurs at a given concentration is of importance as the reference for all other experimental results. To this end, DSC traces are made with the latent heat peaks shown in Figure 2. Calculations show that the enthalpy of structural phase change is ~139 J/mol. The hysteresis region width, at the cooling rate of 5 °C/min, is less than 0.5°, while the width of the transition is approximately 3°.

The transition region is visually confirmed by both confocal and optical microscopy. As Figure 3 demonstrates, a polydomain liquid crystalline texture, the characteristic mosaic expected of the hexagonal phase,[15] forms on cooling by nucleation and growth. This matches well with the previous observations.[8,16] Striations are also observed to form spontaneously in the cooled sample, which is again typical of hexagonal liquid crystals. They nucleate due to sudden two-dimensional dilations in the plane perpendicular to the principal axis of the columns, where the two-dimensional hexagonal order sets in. The undulations

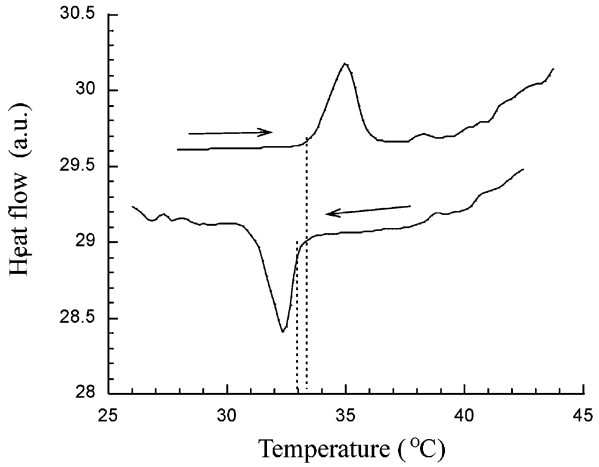

Figure 2. Heating and cooling DSC scans of the 50 wt % TX100−water binary system, obtained at a rate of 5 °C/min. The equilibrium transition point between the isotropic and the hexagonal phase is at $T_c \approx 33$ °C, with a rather narrow hysteresis.

are explained by both a density jump at the phase transition and the decrease of the lattice parameter as temperature decreases.[17] The number of striations per unit volume naturally increases as the cooling rate increases. This deviation from equilibrium cooling forces the formation of more pronounced structures such as zigzag columns in the nonlinear regime.[18] Their presence provides a viable mechanism with which to explain some of the rheological data discussed below. No further treatment of the microscopy is given here; suffice it to say the faster the cooling rate, the greater the degree of supercooling, therefore enforcing more nucleating structures, and the smaller the size of the mosaic domains. This is also of some significance later.

3.2. Cylinder Spacing and Fluctuations. Synchrotron small-angle X-ray diffraction data allow the accurate calculation of the lattice spacing and the periodicity of the hexagonal phase through a range of temperatures. As an illustration, Figure 4a shows the three orders of diffraction peaks obtained at room temperature. Using simple crystallographic arguments, one can verify that these peaks correspond to the {100}, {110}, and {200} planes and that the peak positions in the reciprocal space obey the relationship $1:\sqrt{3}:2$, cf. refs 16 and 19, with the d-spacing of the corresponding planes given by $d = 2\pi/Q$. This provides an excellent confirmation of the hexagonal phase with a calculated lattice parameter $a = (2/\sqrt{3})d_{100} \approx 59.5$ Å at room temperature (which is approximately 15 Å higher than that reported by Galatanu et al.[11]).

Another feature of this phase transformation, apparent from the data in Figure 5a, is the rapid change in the effective lattice spacing in the vicinity of the transition point T_c. Such a sensitivity to temperature, and presumably concentration as well, is a signature of high fluctuations during the phase transition, despite its nominally first-order discontinuous nature. In particular, the sharp variation of lattice spacing a near T_c can be explained by the increase in the amplitude of lateral thermal vibration in the transition region, causing the effective spacing to increase. This is also accompanied by the lower intensity

(13) Marsden, S. S.; McBain, J. W. *J. Phys. Colloid Chem.* **1948**, *52*, 110.
(14) Ekwal, P.; Mandell, L.; Fontell, K. *Mol. Cryst. Liq. Cryst.* **1969**, *8*, 157.
(15) de Gennes, P. G.; Prost, J. *Physics of Liquid Crystals*; Clarendon Press: Oxford, 1993.
(16) Laughlin, R. G. *The Aqueous Phase Behaviour of Surfactants*; Academic Press: London, 1994.
(17) Clunie, J. S.; Goodman, F. F.; Symons, P. C. *Trans. Faraday Soc.* **1969**, *65*, 287.
(18) Oswald, P.; Gérminard, J. C.; Lej_ek, L.; Sallen, L. *J. Phys. II* **1996**, *6*, 281.
(19) Hahn, T. *International Tables for Crystallography*; D. Reidel Publishing Co.; Netherlands, 1983; Vol. A.

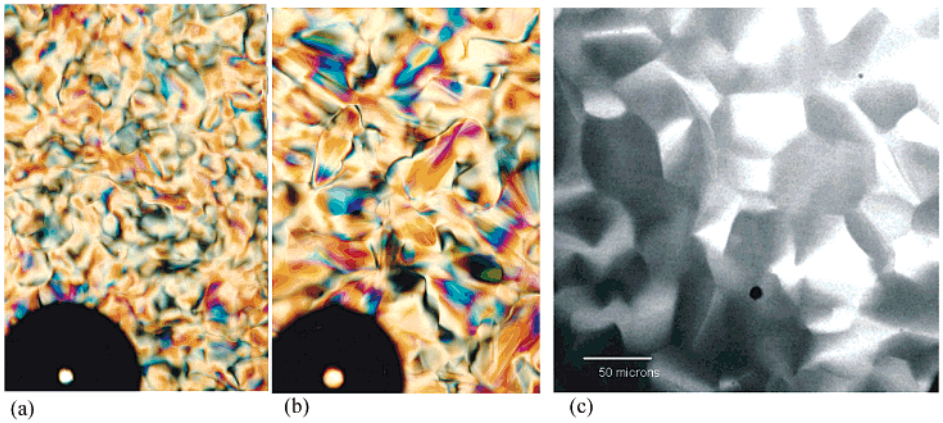

Figure 3. Microscopic textures of the 50 wt % TX100−water binary system. The images in (a) and (b) are from the polarized microscope and show the texture and the striations at the surface of the hexagonal phase obtained by cooling to room temperature at a fast rate of 20 °C/min (a) and at a slow rate of 5 °C/min (b); the reference air bubble indicates exactly the same position in the sample after two cooling cycles. The image in (c) is the confocal microscopy slice through the texture ~100 μm below the free surface; importantly, this texture does not visibly change under the oscillating shear of $\dot{\epsilon} = 0.5\ s^{-1}$. The scale bar of 50 μm applies to all images.

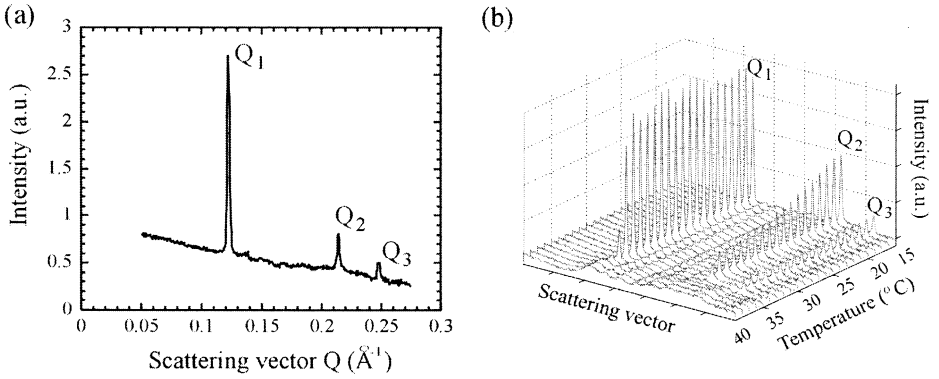

Figure 4. Small-angle X-ray scattering results. (a) A typical raw intensity profile deep in the hexagonal phase, at 20 °C, showing the peaks corresponding to {100}, {110}, and {200} reflections (the ratio $Q_1/Q_2/Q_3 = 1:\sqrt{3}:2$). (b) The evolution of structure on cooling from the isotropic phase. A small broad peak at Q_1 above $T_c \approx 33$ °C is an indication of spherical micellar aggregation; after the phase transition, the relevant reflections rapidly grow in intensity but hardly move in the reciprocal space.

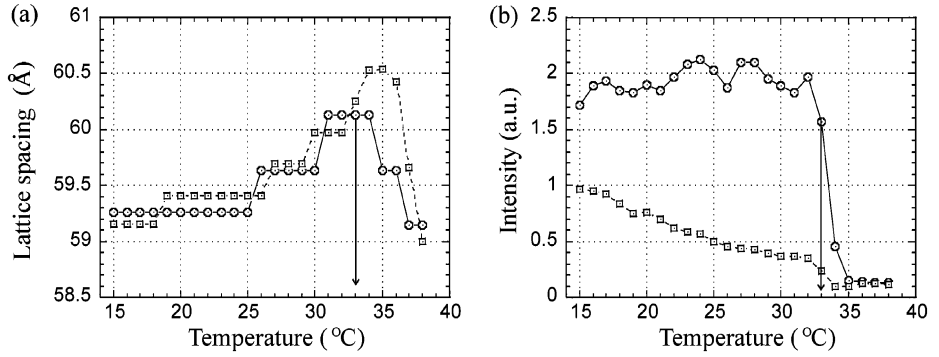

Figure 5. Small-angle X-ray scattering analysis as a function of temperature. (a) The hexagonal lattice spacing a determined from the primary {100} peak position, $a = (2/\sqrt{3})d_{100}$, circles, and from the secondary peak, $a = 2d_{110}$, squares. (b) The intensity of the primary peak (Q_1, circles) and the secondary peak (Q_2, squares). On both plots, the arrow indicates the transition point T_c as determined by DSC.

of the scattering peak {200} with respect to its analogue {100}: a classical Debye−Waller reduction, Figure 4b. Once the region of enhanced critical fluctuations is passed, below around 31 °C, the lattice spacing settles at a relatively constant value and the primary peak intensity saturates as well, indicating a stabilization of order in the hexagonal phase.

One should also note a parallel set of data for the secondary peak ($Q_2 = 2\pi/d_{110}$) on both plots in Figure 5. Although qualitatively the results are the same as for the primary peak, there is a subtle difference. The effective hexagonal lattice spacing calculated from this reflection, $a = 2d_{110}$, shows a more pronounced increase at the critical point. There is also a continuous increase in the peak intensity, unlike that for {100} and {200} reflections. Indeed, these results repeat for all studied samples. A crude initial suggestion could be that the two-dimensional hexagonal mean field affects the cross-section shape of cylinders and makes their transverse fluctuations anisotropic, so that the {100} and {110} directions have a

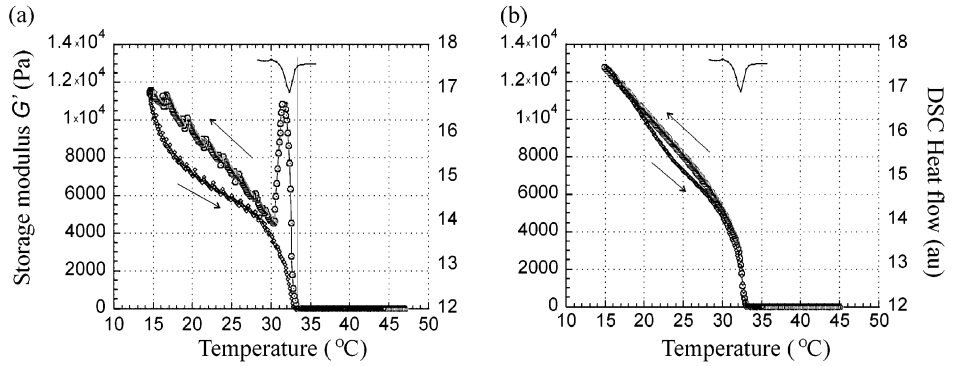

Figure 6. Characteristic elastic response, the storage modulus G', at a frequency of 1 Hz, a strain amplitude of ~1.5%, and a medium rate of temperature change of 0.7 °C/min, obtained on (a) a stress-controlled rheometer and (b) a strain-controlled rheometer. Arrows indicate cooling and heating directions. The anomalous peak on cooling through the phase transition boundary in the plot in (a) is replaced by the critical behavior $G' \propto |T - T_c|^{0.4}$ in (b). Both graphs also show the DSC peak (on cooling, cf. Figure 2) to indicate the position of the transition.

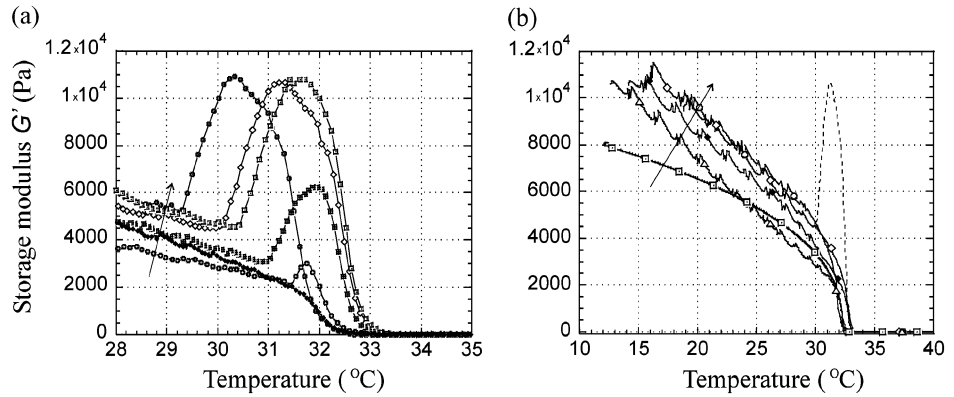

Figure 7. (a) The transition peak in $G'(T)$, obtained on a stress-controlled rheometer, for different cooling rates increasing from 0.1 to 0.4, 0.6, 0.7, 0.8, and 1 °C/min (increasing values are indicated by the arrow in the plot). On increasing the rate, the peak becomes more pronounced, saturates in amplitude, and then shifts to lower temperatures. (b) The evolution of shear modulus with increasing order parameter (on cooling) for the same set of increasing cooling rates (indicated by the arrow) with the transition peak not plotted, mimicking the result of Figure 6b on a strain-controlled rheometer (the dashed line shows the typical transition peak for reference). The low-rate curve (0.1 °C/min, squares), which did not have a transition peak at all, has a very different behavior at lower temperatures as well.

different fluctuation spectrum, the latter changing gradually on cooling and increasing the order parameter. Of course, substantially more work needs to be done if any useful conclusions are to be made regarding this behavior.

4. Rheology at the Phase Boundary

Rheological experiments, central to this work, are conducted in two parts. The first series of tests involves observing the elastic storage modulus response as a function of temperature, at different cooling rates from the isotropic phase. This provides information about the phase transition and the onset and further increase of order in the system. The second test focused on the variation of the response modulus with increasing amplitude of the oscillating strain (at fixed values of frequency and temperature), providing detailed information about shear alignment of the hexagonal phase.

4.1. Effect of Cooling Rate: Transition Kinetics. In this experimental protocol, the material is heated well into the isotropic phase and presheared to ensure the same thermal and mechanical history of all samples. Then the samples are cooled through their phase transition zone at a specified and well-controlled temperature rate, maintaining the constant oscillating shear of amplitude 1.25−1.5% and the constant frequency of 1 Hz. A typical result is illustrated in Figure 6. The plot in Figure 6a, obtained on the stress-controlled rheometer, has a striking feature, namely, the anomalous peak between 33 and 31 °C. Further cooling and subsequent heating show the expected hysteresis loop. However, the anomalous peak around 32 °C in the cooling cycle is not present when the sample is reheated.

This has to be contrasted with the results obtained for the same sample and thermal history and at the same cooling rates but using a strain-controlled rheometer, Figure 6b. The difference in the data acquisition process is briefly outlined in section 2 and, remarkably, leads to very different results. No peak is found on cooling through the phase transition boundary; instead, the storage modulus increases in a "critical" fashion, consistently giving $G' \propto |T - T_c|^{0.4}$ from fitting the data in the vicinity of T_c.

Different cooling rates have been applied and provide two separate observations, summarized in Figure 7a. First of all, as the cooling rate is increased, the transition peak height increases until it saturates at around 1.15×10^4 Pa at a rate of 0.7 °C/min; even higher cooling rates cause the peak to shift to lower temperatures. This is an expected consequence of faster quenching, when both the strength of the transition and the degree of supercooling should increase. Another conclusion can be drawn from comparing the data at low cooling rates, in both parts a and b of Figure 7. At the lowest rate, below 0.1 °C/min, no transition peak can be detected at all. However, the initial growth of G' in the transition region is faster and, for instance,

the modulus is higher than G' at 0.4 °C/min after the "yielding" event in the transition region. On a more extended temperature scale in Figure 7b, one can clearly notice the different slope of $G'(T)$ for the lowest cooling rate, in contrast to all other curves that are obtained in the conditions when the transition peak has been observed.

These findings, consistently reproduced in many repeated experiments, make us suspect that the difference in the rheological response on crossing the phase boundary, obtained on two different rheometers, Figure 6, is not an instrumental artifact but a real physical phenomenon.

One has to re-examine the forces applied to the system in each of the two rheometers. In the strain-controlled method, the fixed amplitude of oscillating rotation angle is provided by the mechanism, generating a corresponding fixed shear strain between the plates of the rheometer. The device then measures the transmitted torque, thus providing the shear stress; the complex modulus $G(\omega)$ is, by definition, the ratio of the two. In the stress-controlled method, the mechanism provides a certain value of torque to the rheometer plate (which can be directly converted to the stress) and measures the resulting rotation angle, converted to the shear strain. In the isotropic phase, the surfactant solution is liquid and very little torque is required to provide the strain amplitude of 1.5%, resisted only by the viscous drag (measured viscosity $\eta \approx 0.025$ Pa s). On the onset of hexagonal phase, at $T = T_c$, a rigid structure is formed in the system, providing a substantial elastic response. In the strain-controlled rheometer, the cell continues to be sheared with the same amplitude, possibly disrupting the initially fragile structures formed at the transition and subsequently providing continuous consistent readings that may not be a true reflection of what is taking place during the phase transition. In contrast, the stress-controlled rheometer still provides a very weak torque, which would no longer be sufficient to distort the "solidifying" system. Then, inevitably with a delay, the software control will detect the decreasing measured strain and will signal to increase the torque supplied to the system; this will gradually increase to the level required to reach the set strain of 1.5%. Accordingly, in the system undergoing a first-order phase transformation, there will be less disruption of the emerging structure and the effectively higher modulus will be reported. As the temperature lowers further and the rigidity of the system increases, the applied torque (stress) will increase further and finally reaches the level at which the initial texture formed at the phase transition yields. The response function drops rapidly, providing the characteristic peak. The delay in disrupting the fragile equilibrium texture will, of course, be more pronounced at higher cooling rates, which corresponds to the observations. At the lowest cooling rate, presumably, the delay in stress adjustment is not sufficient and one essentially always applies the fixed strain to the system; the response has no peak and is identical to that provided by the strain-controlled instrument, which always keeps the system in the dynamic conditions.

There are two factors that contribute to the mechanism of yield behavior, represented by the peaks and the further growth of the shear modulus $G'(T)$. As the cooling rate is increased, the liquid crystalline domain nucleation is enhanced and the resulting polydomain texture is of a smaller size. This is a usual result, confirmed in our case by optical microscopy (see e.g. Oswald et al.[10]). One also expects to find a higher elastic modulus in a smaller texture, due to the increased number of constraints due to domain boundaries. Indeed, we see consistently higher values of G' at higher cooling rates. However, this does not explain why the peaks at the phase transition are formed or why such peaks are not observed, for instance, for lamellar materials (see ref 20). A lamellar phase also forms polydomain textures with dislocations and layer undulations playing a role in rheological response, but we have found no yield peaks in the same conditions as we have seen in the hexagonal phase.

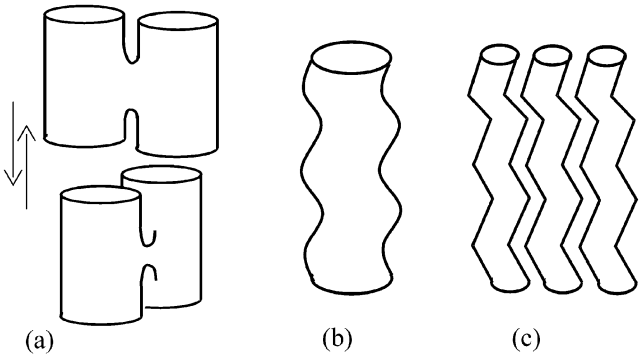

Figure 8. Sketches of (a) the column defects and their locking, (b) column undulations, and (c) zigzag shapes. All these defects, formed in the transition region, should enhance the elastic rigidity of the forming hexagonal lattice.

The experimental evidence suggests a defect locking mechanism in the highly fluctuating transitional regime during the formation of the hexagonal phase. The concentration of imperfections (defects at domain boundaries) increases at higher cooling rates, which would strengthen the structure by defects locking with each other, for instance, as shown in Figure 8a. This in turn causes the high rigidity and subsequent yielding as higher stress is reached, thus producing the observed peaks. Theoretical models also suggest that column undulations play a role,[18,21] Figure 8b. In particular, Prost[22] gives an account of how undulations are able to entangle with each other, therefore increasing the modulus of a system by orders of magnitude.

Another similar idea briefly introduced earlier is the formation of more pronounced nonequilibrium structures such as zigzag columns; see Figure 8c. An increased cooling rate causes greater deviation from equilibrium structures being formed and leads to zigzag-column formations above a critical threshold. Further work needs to be undertaken if one is to detect the characteristic length (λ) of the zigzag in our material, but we can make speculations using conclusions made by Oswald et al.[18] Namely, if in this case λ is comparable to the lattice spacing (60 Å) then it is possible for zigzag columns formed in the nonlinear regime to lock themselves against each other into a rigid metastable structure.

Both ideas assume that defects do not move by permeation during any deformation processes but instead yield above a critical level of stress, leading to a more compliant polydomain texture, susceptible to further shear alignment. Presumably, at the lowest cooling rate, a closer approach to equilibrium is followed and neither defect locking nor the subsequent texture yielding occur, also leading to a visibly different dependence $G'(T)$ at lower temperatures, Figure 7b. This would also explain why the yielding phenomenon does not take place so profoundly in the lamellar phase: it is topologically very difficult to cause the undulation locking in a system of plane layers.

(20) Petrov, P. G.; Ahir, S. V.; Terentjev, E. M. *Langmuir* **2002**, *18*, 9133.
(21) Sallen, L.; Oswald, P.; Gérminard, J. C.; Malthête, J. *J. Phys. II* **1995**, *5*, 937.
(22) Prost, J. *Liq. Cryst.* **1990**, *8*, 123.

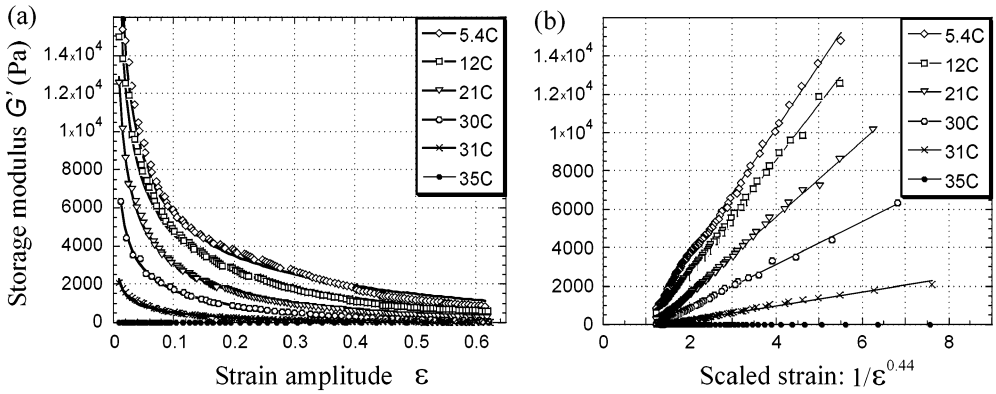

Figure 9. The change in the measured storage modulus G' as a function of the applied strain amplitude ϵ, at a fixed frequency of 1 Hz and temperatures decreasing from 35 °C (in the isotropic phase, $T_c \approx 33$ °C) to 5.4 °C, labeled on the plots. The plot in (a) is essentially the raw data, fitted by the power law $G' = A\epsilon^{-0.44}$; the plot in (b) is emphasizing the linear relations between G' and $1/\epsilon^{0.44}$.

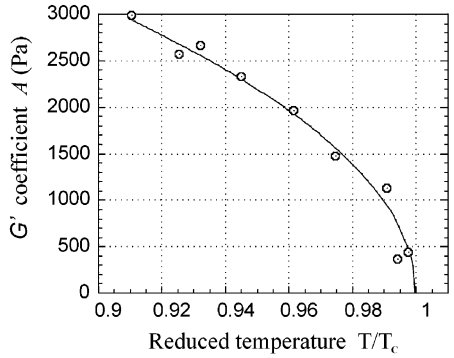

Figure 10. The parameter A, giving the slopes of the linear fits in Figure 9b, plotted against the reduced temperature T/T_c. The solid line shows a fitting by the square-root: $A \propto |1 - T/T_c|^{0.5}$.

Clearly, further experimentation and subsequent analysis need to take place to make more firm conclusions on the unusual rheological signature of the hexagonal phase transition.

4.2. Effect of Strain Amplitude: Shear Alignment. For the second series of experiments, Figure 9a provides a useful illustration of the elastic G' response as the strain amplitude is increased for various temperatures. All samples studied in the series were cooled at the medium rate of ~0.7 °C/min from the presheared isotropic state to the fixed temperature of observation. Accordingly, all samples have gone through the stage of rigid structure formation and yielding, leading to the peak response described in the previous section.

The fitting of experimental data for $G'(\epsilon)$ shows that the modulus clearly follows a power law dependence,

$$G' = A\epsilon^{-0.44} \tag{1}$$

where ϵ is the amplitude of the oscillating strain. The material parameter A is a function of temperature, which is shown by Figure 10. The temperature dependence of this parameter closely follows a critical relationship,

$$A = 9814|1 - T/T_c|^{1/2} \quad \text{(in units of Pa)} \tag{2}$$

However, at this stage it would be premature to assign any special significance to such a behavior: although it resembles a universal critical exponent, one must remember that we are dealing with the first-order phase transformation from the isotropic phase. Additional studies, at different concentrations (thus crossing the phase boundary at a different point) and at different cooling rates (in this way establishing the role of the transition kinetics), need to be performed before any theoretical conclusions are drawn.

The underlying reason for the nonlinear stress−strain response, clearly expressed by the strain dependence of the calculated storage modulus, $G' = A\epsilon^{-0.44}$ from the fitting of data in Figure 9 at all temperatures in the hexagonal phase, is the shear alignment of the polydomain texture. This has been thoroughly discussed in the literature in relation to the lamellar and the hexagonal phases.[5,6,22,23] The reader must note that the region of strains we consider in this work is very low, in comparison with, for example, that of refs 5 and 6. Accordingly, we are never in the regime of complete or substantial alignment, only during the initial onset of it. This has also been confirmed by the optical observation of textures on our confocal microscope equipped with a transparent shear cell. The polydomain texture, shown in Figure 3c, does not visibly change at all for the whole region of strain amplitudes up to our maximum $\epsilon = 65\%$.

The general observation of the falling modulus $G'(\epsilon)$ is consistent with the set of curves in Figure 7b. Except for the lowest cooling rate case (where, clearly, a very different texture occurs), the storage modulus is lower for the lower cooling rate, which means lower defect concentration and more aligned texture. It is important to examine the secondary signature of shear alignment, occurring at the small strain amplitudes. Figure 11a shows the simultaneous plot of the measured shear stress applied to the sample and the $G'(\epsilon)$ variation (the same as in Figure 9a, for 5.4 °C). As the amplitude of the oscillating strain increases, the modulus falls and the stress follows a "quasi-linear" dependence $\sigma = G'(\epsilon)\,\epsilon$. This is proven by plotting a model curve,

$$\sigma = A\epsilon^{0.56} \tag{3}$$

(with the coefficient taken from the fitting of $G'(\epsilon)$ at this temperature), which matches well with the raw data for stress $\sigma(\epsilon)$. This effect is reproducible for all temperatures at which the stress−strain data were collected.

However, above a certain value of strain amplitude, which we label ϵ^* in Figure 11a, the regime of shear alignment clearly changes. One can no longer apply the quasi-linear relationship $\sigma = G'(\epsilon)\,\epsilon$. The values of the threshold strain ϵ^* are obtained for all temperatures and

(23) Hadziioannou, G.; Mathis, A.; Skoulios, A. *Colloid Polym. Sci.* **1979**, *257*, 136.

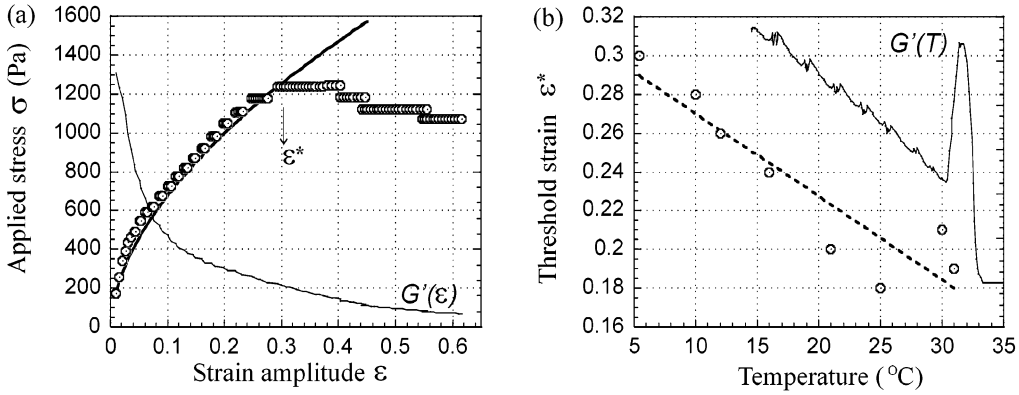

Figure 11. (a) The simultaneous plot of the measured applied stress σ (data points), depending on the strain amplitude, and the shear modulus $G'(\epsilon)$ (thin line) as in Figure 9a, for a single temperature, 5.4 °C. The full solid line shows the model $\sigma = A\epsilon^{0.56}$. (b) The values of threshold strain amplitude ϵ^*, obtained for different temperatures; the dashed line is a guide for the eye. The thin line shows the typical shear modulus $G'(T)$ data for reference.

are plotted in Figure 11b. We have no explanation for the apparent drop in the measured stress $\sigma(\epsilon)$, which is still more confusing since, one presumes, the rheometer *calculates* the value of G' from the measured σ and ϵ data. It is clear that kinetic effects play a role, similar to the effect of the G' peak in the previous section. Since the shear alignment is a function of shear rate (not just the shear amplitude ϵ^*), one presumes that at a threshold value of $\dot{\epsilon} = \omega\epsilon^*$ a new dynamic regime sets in. In fact, Ramos et al.[6] have recently shown the flow curves of a swollen hexagonal phase and demonstrated a very similar threshold in their stress−strain rate dependence. However, their value for the threshold strain rate ($\dot{\epsilon} \sim 100\ s^{-1}$) is very much higher than in our case (at a frequency $\omega =$ 1 Hz, the threshold strain rate is $\sim 0.2\ s^{-1}$); this presumably is due to the highly swollen hexagonal phase in ref 6 and a much more dense packing of cylinders in our case. One can also notice a consistent decrease in the threshold value ϵ^* with temperature, Figure 11b, which should be expected as the hexagonal order parameter decreases, resulting in the decrease in all elastic barriers for domain alignment.

In the dynamic alignment regime above the threshold ϵ^*, one finds the increasing role of a plastic flow in the material. This may offer some significant insight into the nature of the structural change. As suggested by Schmidt et al. and Ramos et al.[5,6] for other surfactant solutions, once a certain critical point is reached, the material yields, allowing flow to become the dominant process in microstructural change. Application of shear makes the principal axis of the micellar rods align parallel to the velocity[23,24] but also causes a loss of the long-range two-dimensional hexagonal order in the system. In this state, the material is much more vulnerable to the creep flow and thus the G' response tends gradually toward zero.

5. Conclusions

The Triton X100/water binary system has presented some curious rheological results that have been discussed in this paper. Typical structural results and texture patterns have been observed alongside more novel yielding and strain-threshold results. From a large length scale perspective, the polydomain texture was analyzed using both confocal and ordinary polarized microscopy techniques; it confirms the presence of defects such as striations during the specified temperature and shear regimes. In itself, this would not seem too significant, but confirming their presence is of great importance when considering the rheological results.

The small-angle X-ray data suggest that the hexagonal lattice parameter is ~60 Å. A plot of the intensity of the second peak (Q_2, {110}) against temperature also reveals a more subtle result, showing that its intensity does not abruptly collapse at the first-order phase transition but gradually declines as the temperature is increased toward T_c. This suggests that fluctuations in the hexagonal system are highly anisotropic and some crystallographic systems have more freedom to move, over a much wider range of temperatures.

However, of most significance to us is the behavior of the hexagonal phase during the rheological scans across the phase boundary. This provides a new dimension to studying the phase equilibrium and kinetics of complex fluids. Varying cooling rates and observing a rheological response as the material is taken through its phase transition has isolated what we have termed "yield peaks". The formation of rigid but fragile structures at the phase transition is believed to be due to different types of defects including dislocations and cylinder bridging. However, the effects of fluctuations, in the form of cylinder undulations or zigzags, may also have a significant role in the phase transition rheology.

Stress−strain experiments at a fixed temperature have also provided useful insight into the shear-induced evolution of polydomain hexagonal structures. The results have shown very clearly that consistent trends and well-defined laws can be applied to the onset of shear alignment in the material. We also find a critical threshold strain (rate) above which the regime of nonlinear elastic response, characterized by the relation $\sigma = G'(\epsilon)\,\epsilon$, changes to a strongly pronounced creep and plastic flow. However, it is not yet clear whether the observed phenomenological relations are universal. For instance, does the exponent of critical temperature dependence $G' \propto (T - T_c)^{0.4}$ obtained in the strain-controlled rheometer depend on binary mixture concentration (that is, the distance away from the transition point on the phase diagram)? Is the unambiguous power law $G' \propto \epsilon^{-0.44}$ on initial (elastic) stages of shear alignment a function of concentration too, and, accordingly, of the size of cylindrical micelles? How well reproducible is the threshold strain $\epsilon^*(T)$ when the material has been cooled at different rates? Questions such as these require much more experimental work to establish a firm platform for theoretical analysis.

(24) Fredrickson, G. H.; Bates, F. S. *Annu. Rev. Mater. Sci.* **1996**, *26*, 501.

Acknowledgment. We thank F. Baker, A. R. Tajbakhsh, S. Mistry, and M. Myatt for useful discussions and guidance. The help of J. Sanderson, in obtaining the SAXS X-ray data from the Daresbury synchrotron radiation source, of I. Hopkinson and L. Kershaw, in confocal imaging, and of X.-F. Yuan of King's College London, in allowing access to the strain-controlled rheometer, is gratefully appreciated. This work has been supported by EPSRC U.K.

LA025793C